On the use of manometry method for measurement of gas adsorption equilibria and characterization of clay texture with Derivative Isotherm Summation

Denys Grekov, Pascaline Pre, Bernd Grambow

On the use of manometry method for measurement of gas adsorption equilibria and characterization of clay texture with Derivative Isotherm Summation.

Denys Grekov,[a*] Pascaline Pré,[b] Bernd Grambow[a]

[a] SUBATECH (IMT Atlantique, Université de Nantes, CNRS-IN2P3), F-44307 Nantes, France

[b] IMT Atlantique, GEPEA UMR CNRS 6144, F-44307 Nantes, France

Corresponding author: denys.grekov@imt-atlantique.fr

Abstract

Gas adsorption is widely used for characterization of clays. Apart from "classical" experiment of nitrogen or other gases adsorption/desorption at cryogenic temperatures, allowing the determination of the specific surface area, partial mesopore and micropore volume and size distributions, gas adsorption can also be used for the characterization of clay surface texture (energetic heterogeneity) related to layered structure of clays. Derivative Isotherm Summation applied to high-resolution gas adsorption isotherms was shown to be a powerful tool to access energetic characteristics and ratio between basal and lateral faces of clay particles. To date, the method is not commonly employed for characterization of clays and other heterogeneous solids, probably due to specificity of high-resolution isotherms acquisition technique described in the original literature: quasi-equilibrium volumetry with gas injection by microleak. We illustrated in the present work a possibility to use widely available static manometric commercial gas adsorption analysers for this purpose.

Keywords: clay particles; basal faces; lateral faces; gas adsorption; derivative isotherm summation.

1. Introduction

Clay particles feature a specific texture originating from the coexistence of structurally inequivalent basal (pyrophilite-like) and lateral (hydroxylated) faces. These influence properties of clays such as cation exchange capacity, chemical species retention, zeta potential etc. (Bradbury and Baeyens, 2000; Hassan et al., 2005; Leroy et al., 2015). Atomic force microscopy (AFM) and electron microscopy image reconstruction (Ploehn et al., 2000; Tournassat et al., 2003; Cadene et al., 2005; Sayed Hassan et al., 2006) and Derivative Isotherm Summation (DIS) (Bardot et al., 1998; Michot and Villiéras, 2002) have emerged as accurate tools to characterize the texture of clay surfaces. While the former technique is well-known and currently utilized for characterization of clays and other layered solids, the application of the latter one is less common. A detailed description of DIS method can be found in the original literature and reviews (Villiéras et al., 1992, 1997, 2002; Nir et al., 2006). Here we only briefly recall the basic principle of DIS in the context of clays surface characterization.

Michot et al. illustrated that for majority of clays, upon Ar or N_2 adsorption at 77 K, the monolayer completion occurs first on highly polarizing lateral faces (at lower pressures) and then on basal surfaces (at higher pressures) (Michot et al., 1990). Quasi-equilibrium volumetry (or more precisely manometry) with gas injection by micro-leak was proposed for the acquisition of high-resolution isotherms composed of more than 2000 experimental points in the domain of relative pressures ranging between 10^{-7} and 0.1. This technique offers the advantage of detecting progressive monolayer completion on different surface domains and usually allows the acquisition of very smooth isotherms. Villieras et al. have further proposed to simulate the derivatives of high-resolution isotherms, being more sensitive to fine variations of adsorbed amount, especially in the case of multi-component isotherms, with the sum of theoretical monolayer or multilayer adsorption isotherm derivatives in order to access

energetic parameters of adsorption and areas of individual surface domains (DIS procedure) (Villiéras et al., 1992). A very similar procedure for the calculation of adsorption potential distribution was introduced earlier by Jaroniec and Choma (Jaroniec and Choma, 1987) for the characterization of microporous materials (Jaroniec et al., 1996; Jaroniec and Choma, 1997). The most commonly employed models for isotherm simulation in the context of DIS for the characterization of clays are Bragg-Williams-Temkin (BWT) (1) and Brunauer-Emmett-Teller-Hill (BET-H) (2) equations describing monolayer and multilayer adsorption respectively. According to these models, the coverage of adsorption sites θ (related to adsorbed amount V_{ads}) with relative gas pressure (p/p°) is influenced by adsorbate/adsorbent and lateral adsorbate/adsorbate interactions, which are described respectively with the parameters C and ω. More details are given in (Villiéras et al., 1997). Equation (1) is usually retained for the description of low-pressure components. Its derivative in $\ln(p/p^{\circ})$ – $dV_{ads}/d\ln(p/p^{\circ})$ coordinates affords symmetric peaks with the position and width being determined by C and ω respectively. The derivative of equation (2) leads to peaks with ascending right-hand side and is mostly used for the description of high-pressure components where multilayer adsorption takes place. Other models for the description of adsorption on planar surfaces and in micropores (Dubinin-Astakhov equation and its extensions) are also available (Villiéras et al., 1997). Due to its quadrupolar momentum, nitrogen specifically interacts with cations or other chemical species such as surface hydroxyl groups and may be differently oriented near these sites, making isotherm analysis difficult. Thus, monoatomic gases like argon, characterized by spherical geometry are preferred probes for surface texture analysis.

$$\theta = \frac{C \cdot \exp\left(\frac{\omega \cdot \theta}{kT}\right) \cdot exp\left(ln(p/p^{\circ})\right)}{1 + C \cdot \exp\left(\frac{\omega \cdot \theta}{kT}\right) \cdot exp\left(ln(p/p^{\circ})\right)} \quad (1)$$

$$\theta = \frac{C \cdot \exp\left(\frac{\omega \cdot \theta}{kT}\right) \cdot exp\left(ln(p/p^{\circ})\right)}{\left[1 - exp\left(ln(p/p^{\circ})\right)\right] \cdot \left[1 + \left(C \cdot \exp\left(\frac{\omega \cdot \theta}{kT}\right) - 1\right) \cdot exp\left(ln(p/p^{\circ})\right)\right]} \quad (2)$$

DIS was illustrated to be a powerful tool for surface heterogeneity analysis, and it was extensively applied by Villieras and co-authors for the characterization of different families of clays and other minerals and synthetic materials, such as nanocrystalline or microporous solids (Bardot et al., 1998; Michot and Villiéras, 2002; Prélot et al., 2003b, 2003a; Garnier et al., 2007; Ali Ahmad et al., 2013). Nowadays, the DIS technique is not commonly employed, probably due to the specificity of the equipment proposed in the original literature for the acquisition of high-resolution isotherms smooth enough to obtain interpretable derivatives. In the present contribution, we evaluate the applicability of the DIS procedure to high-resolution isotherms obtained with available commercial gas adsorption analysers in the context of clay surfaces heterogeneity analysis, using Argon adsorption at 77 K.

2. Materials and methods

Gas adsorption isotherm measurement. The isotherms were acquired using 3Flex automated static manometric adsorption analyser from Micromeritics, equipped with high accuracy pressure transducers (precision 0.15 % of absolute pressure reading) allowing for measurements in the domain of Argon or Nitrogen relative pressure ranging between 10^{-6}-10^{-7} and 1. Such a broad range of pressures is required for characterization of micro- and mesopores. The acquisition was performed in fixed-dose mode, varying the amount of injected gas between 0.01 and 10 cm^3/g, depending on pressure interval and specific surface area of analysed samples. In the same way, the equilibration time after gas injection was adjusted and optimized by varying the pressure measurement interval from 10 up to 90 s. The optimization procedure consists of the research of experimental conditions where the thermodynamic equilibrium of adsorption is attained and completely smooth isotherm,

95 featuring at least 10-20 points per decade of gas pressure values, is acquired within 48-60 h,
96 which corresponds to the autonomy time of the Dewar vessel filled with liquid nitrogen to
97 maintain cryogenic temperature in the sample tube. As an example, for Illite du Puy featuring
98 specific surface area close to 100 m^2/g we found the following amounts of injected Ar
99 allowing the generation of sufficiently high number of experimental points per domain of
100 values of gas pressures: 0.015 cm^3/g until $p/p°=2\cdot10^{-5}$, then 0.05 cm^3/g until $p/p°=2\cdot10^{-4}$, then
101 0.15 cm^3/g until $p/p°=10^{-3}$, then 0.2 cm^3/g until $p/p°=10^{-2}$, 0.6 cm^3/g until $p/p°=10^{-1}$ and
102 finally 5 cm^3/g until $p/p°=3\cdot10^{-1}$. Pressure measurement interval during equilibration
103 processes was set to 15 s for relative pressures ranging between $2\cdot10^{-5}$ and $3\cdot10^{-1}$, its
104 prolongation did not significantly influence the isotherm shape. Since at low pressure the
105 equilibration kinetics is slow this parameter was fixed to 30 s below $p/p°=2\cdot10^{-5}$ in order to
106 avoid s-shaped artefact. The saturated vapour pressure of Argon at 77 K was measured
107 periodically. Specific surface areas were determined from Ar adsorption isotherms using BET
108 theory (adsorbed Ar cross section area at 77 K – 0.143 nm^2) in the domain of relative
109 pressures 0.1-0.3. Before isotherms measurements, all samples were outgassed under dynamic
110 vacuum at 393 K until residual pressure stabilization (at least 72 h). The volumes of cells non-
111 occupied by samples were determined at ambient temperature and at 77 K by He expansion.

112 The derivatives of experimentally measured isotherms were calculated using numerical
113 procedure. Only smooth isotherms afford “high-quality” interpretable derivatives. Those were
114 simulated with the sum of derivatives determined from the equations (1) and (2). For low-
115 pressure domains, we mainly considered BWT equation (monolayer adsorption) while for
116 high-pressure domain, where multilayer adsorption takes place – BET-H equation. Both
117 equations were resolved using an iterative method for each experimentally measured point of
118 pressure whilst their derivatives were computed by differentiation. The number of
119 components needed to simulate experimental isotherm derivatives, their weight and

parameters C and ω were adjusted as best-fit parameters minimising the residual sum of squares between experimental and simulated isotherms, as recommended in (Villiéras et al., 1997). The weight of the individual components corresponds to their contribution to the total specific surface area of the solid. In the specific case of clays, the contribution (fraction) of surfaces of basal faces to the total specific surface area (composed of basal and lateral faces) corresponds to the lamillarity index (L) which quantitatively describes their texture.

Sample preparation. A fine (< 2 µm) montmorillonite fraction was extracted from Bentonite MX-80 by 5 g/l suspension centrifugation at 1000 rpm and it was further exchanged with Na by following the standard procedure: contact with 0.5 mol/l NaCl solution, 6 cycles of centrifugation at 20000 rpm and subsequent washing/re-dispersion in deionized water and suspension drying at 323 K under air. The clay fraction from Illite du Puy was purified by an elutriation procedure and further transformed to a Na-exchanged form in the same way as a montmorillonite sample (Tournassat et al., 2007). Kaolinite was received from Fluka Analytical (Sigma Aldrich) in form of fine powder (<150 µm) and analysed without any purification. Two core samples of natural clay-rock come from the Callovo-Oxfordian mudstones, East of Paris basin, underground laboratory of Bure, France (Gaucher et al., 2004). Both samples are characterized by the same clay fraction content (about 45%) featuring different composition (COx-EST 48599 (-508,3 m): 75-80% of illite and 20-25% of smectite, COx-EST 48601 (-466 m): 60-70% of illite and 30-40% of smectite). All samples except kaolinite (already powdered) were grinded manually and sieved to collect < 100 µm size fraction.

3. Results and discussion

In a first step high-resolution Ar adsorption isotherms were acquired for three pure-phase "model" clays: kaolinite, illite and montmorillonite, extensively studied by the DIS technique (Villiéras et al., 1997; Bardot et al., 1998; Tournassat et al., 2003; Sayed Hassan et al., 2006).

145 The experimental isotherms and their derivatives are shown in Figure 1. All isotherm
146 derivatives feature a classical shape as observed earlier, including a major component
147 characterized by a peak at ln(p/p°)≈ -4..-5 and a more or less pronounced secondary
148 component in the range of lower pressures, merging as a shoulder at ln(p/p°)≈ -8..-6, as well
149 as a minor component below -10. Isotherm deconvolution with BWT and BET-H models
150 reveals an overlap of these different contributions. According to the bibliographic results
151 (Sayed Hassan et al., 2006), low-energy (high-pressure) and high-energy (low-pressure)
152 components are assigned, with some exceptions (Villiéras et al., 1997, 2002), to basal (b) and
153 lateral (l) faces respectively. The lamellarity index (L) determined by the degree of layers
154 stacking is used for quantitative description of clays texture. For kaolinite and illite the shapes
155 of isotherms and deduced energetic parameters of argon adsorption on different surface
156 domains (C and ω) are close to those reported in the literature (Table 1) (Sayed Hassan et al.,
157 2006). For montmorillonite extracted from bentonite MX-80, however, the isotherm envelop
158 slightly differs: low-pressure components, related to the contribution of lateral faces, feature a
159 more pronounced character when compared to that described by Tournassat et al. (Tournassat
160 et al., 2003). A similar signature was observed for Na-SWy-1 montmorillonite (Le Forestier et
161 al., 2010). The difference in textural properties of montmorillonites can be related to sample
162 preparation procedure. In the present work clay suspension was air dried while in (Tournassat
163 et al., 2003) it was freeze-dried and according to (Pacuła et al., 2006), freeze-drying may
164 influence surface areas and texture of swelling clays.

165 We further probed the use of equilibrium manometry for high-resolution Ar adsorption
166 isotherms acquisition for natural clay rock samples texture analysis. Isotherm derivatives
167 together with their best-fit simulation (BWT and BET-H models) for COx-EST 48599 and
168 COx-EST 48601 argillite are represented in Figure 2. The shapes of the isotherms are similar
169 to those of pure-phase clays. In spite of the closeness of structural features of single-phase

clays and argillite clay fraction (Tournassat et al., 2009), the components of the isotherms accessed by best-fit simulation are assigned to the same surface sites as in cases of reference systems, i.e. low-pressure components – lateral faces, high-pressure components – basal faces. While low-pressure components of both isotherms feature almost identical intensity, the high-pressure main component in case of COx-EST 48601 isotherm is less pronounced in comparison to COx-EST 48599. This suggests a lower contribution of basal faces to the total specific surface area for former argillite. Energetic parameters determined by isotherm simulation are summarized in Table 1.

Comparing the lamellarity indexes for pure-phase clays, one can realize that in case of montmorillonite sample, characterized by low value of L and consequently low contribution of basal faces to the total specific surface area (Table 1), the stacking of phyllosilicate sheets is higher than for illite or kaolinite featuring higher L values. Interestingly, the same trend is also observed for natural clay rock samples. For instance, COx-EST 48601, which features higher smectite fraction content, is characterized by lower lamellarity index and thus higher level of phyllosilicate sheets stacking acquired during diagenesis in comparison to COx-EST 48599.

4. Conclusion

High-resolution Ar adsorption isotherms were acquired at 77 K for a series of model single-phase clays and complex natural argillite samples using static manometry method. High-quality derivatives were obtained for the entire set of samples despite significantly lower number of measured experimental points (on the order of 150-250) in comparison to isotherm acquisition by quasi-equilibrium manometry with gas injection by micro-leak (more than 2000 points). Simulation of measured isotherms derivatives with the sum of derivatives of theoretical isotherms computed with the BWT and BET-H models afforded energetic parameters and areas of basal and lateral faces of clay particles. The shapes of measured

isotherms, energetic parameters and textural properties accessed for model single-phase clays were found to be in a good agreement with those for similar systems described in the literature. This illustrates a possibility of using commercial gas adsorption analysers for clays surfaces texture characterization by DIS technique, making indeed the method more accessible. By analysing natural clay rock samples with this approach, we confirmed the relationship between illite/smectite ratio and the degree of phyllosilicate layer staking, quantitatively described by lamellarity index. One should notice that a possibility of natural argillite texture characterization without specific sample preparation is a great advantage of DIS in comparison to AFM image reconstruction technique.

Acknowledgements

The present work was supported by the industrial chair "Storage and Disposal of Radioactive Waste" at the Institut Mines-Télécom Atlantique, funded by ANDRA, Orano, and EDF.

References

Ali Ahmad, M., Prelot, B., Dufour, F., Durupthy, O., Razafitianamaharavo, A., Douillard, J.M., Chaneac, C., Villiéras, F., Zajac, J., 2013. Influence of morphology and crystallinity on surface reactivity of nanosized anatase TiO2 studied by adsorption techniques. 2. solid-liquid interface. J. Phys. Chem. C 117, 4459–4469. https://doi.org/10.1021/jp3077084

Bardot, F., Villiéras, F., Michot, L.J., François, M., Gérard, G., Cases, J.M., 1998. High resolution gas adsorption study on illites permuted with various cations: Assessment of surface energetic properties. J. Dispers. Sci. Technol. 19, 739–759. https://doi.org/10.1080/01932699808913212

Bradbury, M.H., Baeyens, B., 2000. A generalised sorption model for the concentration

218 dependent uptake of caesium by argillaceous rocks. J. Contam. Hydrol. 42, 141–163.
219 https://doi.org/10.1016/S0169-7722(99)00094-7

220 Cadene, A., Durand-Vidal, S., Turq, P., Brendle, J., 2005. Study of individual Na-
221 montmorillonite particles size, morphology, and apparent charge. J. Colloid Interface
222 Sci. 285, 719–730. https://doi.org/10.1016/j.jcis.2004.12.016

223 Garnier, C., Görner, T., Villiéras, F., De Donato, P., Polakovič, M., Bersillon, J.L., Michot,
224 L.J., 2007. Activated carbon surface heterogeneity seen by parallel probing by inverse
225 liquid chromatography at the solid/liquid interface and by gas adsorption analysis at the
226 solid/gas interface. Carbon N. Y. 45, 240–247.
227 https://doi.org/10.1016/j.carbon.2006.10.004

228 Gaucher, E., Robelin, C., Matray, J.M., Négrel, G., Gros, Y., Heitz, J.F., Vinsot, A., Rebours,
229 H., Cassagnabère, A., Bouchet, A., 2004. ANDRA underground research laboratory:
230 Interpretation of the mineralogical and geochemical data acquired in the Callovian-
231 Oxfordian formation by investigative drilling. Phys. Chem. Earth 29, 55–77.
232 https://doi.org/10.1016/j.pce.2003.11.006

233 Hassan, M.S., Villiéras, F., Razafitianamaharavo, A., Michot, L.J., 2005. Role of
234 exchangeable cations on geometrical and energetic surface heterogeneity of kaolinites.
235 Langmuir 21, 12283–12289. https://doi.org/10.1021/la051993n

236 Jaroniec, M., Choma, J., 1997. Characterization of geometrical and energetic heterogeneities
237 of active carbons by using sorption measurements. Equilibria Dyn. Gas Adsorpt.
238 Heterog. Solid Surfaces Stud. Surf. Sci. Catal. 104, 715–744.

239 Jaroniec, M., Choma, J., 1987. Characterization of activated carbons by distribution functions
240 of adsorption potential and micropore dimension. Mater. Chem. Phys. 18, 103–117.
241 https://doi.org/10.1016/0254-0584(87)90115-5

242 Jaroniec, M., Gadkaree, K.P., Choma, J., 1996. Relation between adsorption potential
243 distribution and pore volume distribution for microporous carbons. Colloids Surfaces A
244 Physicochem. Eng. Asp. 118, 203–210. https://doi.org/10.1016/S0927-7757(96)03685-0
245 Le Forestier, L., Muller, F., Villieras, F., Pelletier, M., 2010. Textural and hydration
246 properties of a synthetic montmorillonite compared with a natural Na-exchanged clay
247 analogue. Appl. Clay Sci. 48, 18–25. https://doi.org/10.1016/j.clay.2009.11.038
248 Leroy, P., Tournassat, C., Bernard, O., Devau, N., Azaroual, M., 2015. The electrophoretic
249 mobility of montmorillonite. Zeta potential and surface conductivity effects. J. Colloid
250 Interface Sci. 451, 21–39. https://doi.org/10.1016/j.jcis.2015.03.047
251 Michot, L., Francois, M., Cases, J.M., 1990. Surface Heterogeneity Studied by a Quasi-
252 Equilibrium Gas Adsorption Procedure. Langmuir 6, 677–681.
253 https://doi.org/10.1021/la00093a025
254 Michot, L.J., Villiéras, F., 2002. Assessment of surface energetic heterogeneity of synthetic
255 Na- saponites. The role of layer charge. Clay Miner. 37, 39–57.
256 https://doi.org/10.1180/0009855023710016
257 Nir, S., El Nahhal, Y., Undabeytia, T., Rytwo, G., Polubesova, T., Mishael, Y., Rabinovitz,
258 U., Rubin, B., 2006. Handbook of Clay Science, Developments in Clay Science.
259 https://doi.org/10.1016/S1572-4352(05)01021-4
260 Pacuła, A., Bielańska, E., Gaweł, A., Bahranowski, K., Serwicka, E.M., 2006. Textural effects
261 in powdered montmorillonite induced by freeze-drying and ultrasound pretreatment.
262 Appl. Clay Sci. 32, 64–72. https://doi.org/10.1016/j.clay.2005.10.002
263 Ploehn, H.J., Liu, C., Scrivens, W.A., Loye, H., 2000. Quantitative Analysis of Platelet Size
264 by Atomic Force Microscopy 1–4.
265 Prélot, B., Villiéras, F., Pelletier, M., Gérard, G., Gaboriaud, F., Ehrhardt, J.J., Perrone, J.,

Fedoroff, M., Jeanjean, J., Lefèvre, G., Mazerolles, L., Pastol, J.L., Rouchaud, J.C., Lindecker, C., 2003a. Morphology and surface heterogeneities in synthetic goethites. J. Colloid Interface Sci. 261, 244–254. https://doi.org/10.1016/S0021-9797(03)00058-4

Prélot, B., Villiéras, F., Pelletier, M., Razafitianamaharavo, A., Thomas, F., Poinsignon, C., 2003b. Structural–chemical disorder of manganese dioxides. J. Colloid Interface Sci. 264, 343–353. https://doi.org/10.1016/s0021-9797(03)00394-1

Sayed Hassan, M., Villieras, F., Gaboriaud, F., Razafitianamaharavo, A., 2006. AFM and low-pressure argon adsorption analysis of geometrical properties of phyllosilicates. J. Colloid Interface Sci. 296, 614–623. https://doi.org/10.1016/j.jcis.2005.09.028

Tournassat, C., Gailhanou, H., Crouzet, C., Braibant, G., Gautier, A., Gaucher, E.C., 2009. Cation Exchange Selectivity Coefficient Values on Smectite and Mixed-Layer Illite/Smectite Minerals. Soil Sci. Soc. Am. J. 73, 928. https://doi.org/10.2136/sssaj2008.0285

Tournassat, C., Gailhanou, H., Crouzet, C., Braibant, G., Gautier, A., Lassin, A., Blanc, P., Gaucher, E.C., 2007. Two cation exchange models for direct and inverse modelling of solution major cation composition in equilibrium with illite surfaces. Geochim. Cosmochim. Acta 71, 1098–1114. https://doi.org/10.1016/j.gca.2006.11.018

Tournassat, C., Neaman, A., Villéras, F., Bosbach, D., Charlet, L., 2003. Nanomorphology of montmorillonite particles: Estimation of the clay edge sorption site density by low-pressure gas adsorption and AFM observations. Am. Mineral. 88, 1989–1995.

Villiéras, F., Cases, J.M., François, M., Michot, L.J., Thomas, F., 1992. Texture and Surface Energetic Heterogeneity of Solids from Modeling of Low Pressure Gas Adsorption Isotherms. Langmuir 8, 1789–1795. https://doi.org/10.1021/la00043a018

Villiéras, F., Michot, L.J., Bardot, F., Cases, J.M., François, M., Rudziński, W., 1997. An

290 Improved Derivative Isotherm Summation Method To Study Surface Heterogeneity of
291 Clay Minerals †. Langmuir 13, 1104–1117. https://doi.org/10.1021/la9510083

292 Villiéras, F., Michot, L.J., Bardot, F., Chamerois, M., Eypert-Blaison, C., François, M.,
293 Gérard, G., Cases, J.-M., 2002. Surface heterogeneity of minerals. Comptes Rendus
294 Geosci. 334, 597–609. https://doi.org/10.1016/s1631-0713(02)01799-6

295

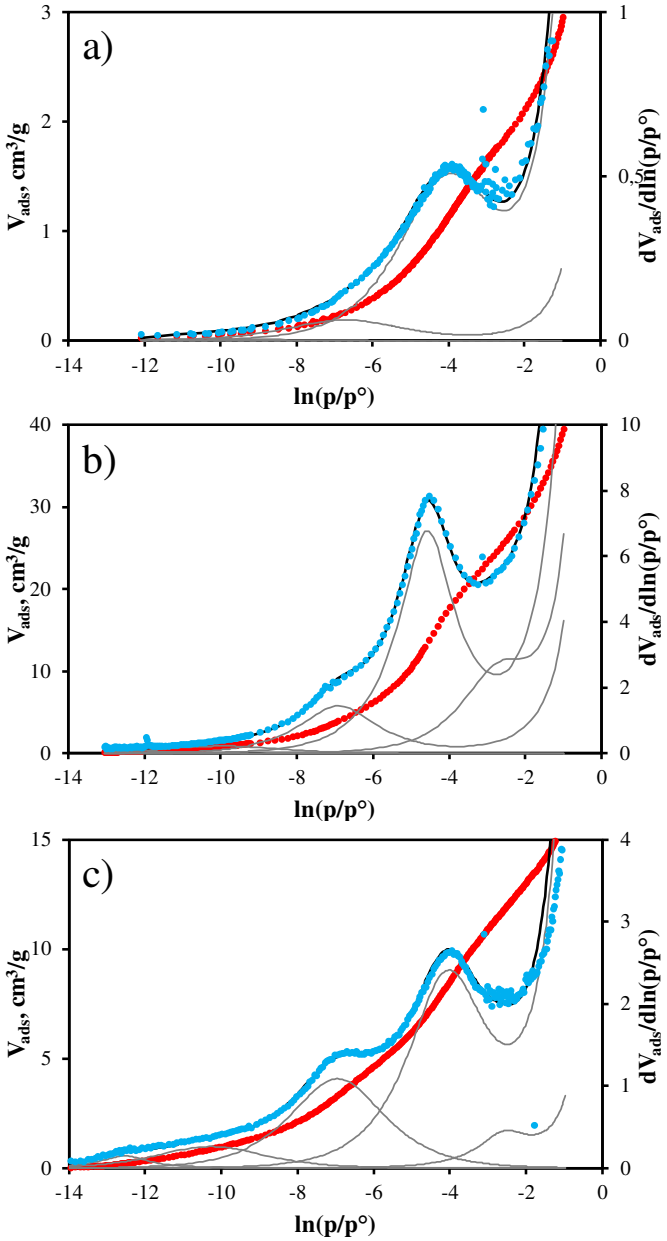

Figure 1. Isotherms (red points) of argon adsorption at 77 K and corresponding derivatives (blue points) together with their best-fit simulations (black line) and individual contributions (grey lines) for: a) kaolinite, b) illite and c) montmorillonite.

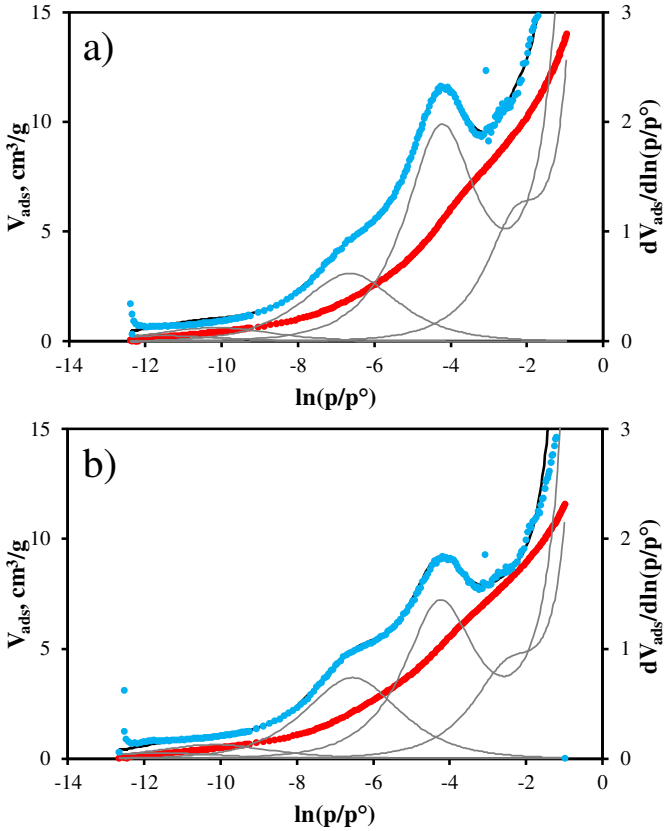

Figure 2. Isotherms (red points) of argon adsorption at 77 K and corresponding derivatives (blue points) together with their best-fit simulations (black line) and individual contributions (grey lines) for: a) COx-EST 48599 and b) COx-EST 48601 clay rock samples.

Table 1. Energetic parameters and areas of different domains of clays surfaces determined by DIS procedure applied to high-resolution Ar adsorption isotherms.

Component	I (b)	II (b)	III (l)	IV (l)	V (l)
Kaolinite (Fluka) S_{BET}=7.6 m^2/g, L=0.85					
Position		-3.7	-6.9	-9.7	
S_i, m^2/g		6.4	1	0.2	
C		44	800	$20 \cdot 10^3$	
ω		0.5	0	0	
***Kaolinite (Kga2) (Sayed Hassan et al., 2006) S_{BET}=21 m^2/g, L=0.84**					
Position	-2.2	-3.8	-6.8	-9.7	
S_i, m^2/g	3.8	13.9	2.3	0.5	
ω	0	1.3	-0.8	0	
Illite du Puy-Na S_{BET}=108 m^2/g, L=0.8					
Position	-2.4	-4.4	-6.9	-10.1	-12
S_i, m^2/g	25	61	16.5	3.6	1.4
C	9	42	550	$20 \cdot 10^3$	$50 \cdot 10^4$
ω	1	1.6	1.1	0	0
***Illite du Puy-Na (Sayed Hassan et al., 2006) S_{BET}=171 m^2/g, L=0.78**					
Position	-2.6	-4.5	-6.9	-10.1	-13
S_i, m^2/g	61.4	71.2	29.7	7.5	0.7
ω	0	1.7	0.5	0	0.5
Montmorillonite-Na S_{BET}=45 m^2/g, L=0.6					
Position	-2.3	-3.9	-6.8	-10.4	-12.6
S_i, m^2/g	2.9	24.1	13.3	3.6	1.1
C	6	35	750	$25 \cdot 10^3$	$10 \cdot 10^4$
ω	1.5	1	0.6	0.2	1
***Montmorillonite SWy-2-Na (Le Forestier et al., 2010) S_{BET}=47 m^2/g, L=0.47**					
Position	-2.7	-4.4	-7	-9.6	
S_i, m^2/g	2.6	19.2	20.6	4.8	
***Bentonite MX-80 (Tournassat et al., 2003) S_{BET}=35 m^2/g, L=0.75**					
Position	-2.5	-4.1	-7	-10.3	
S_i, m^2/g	2	24.6	5.6	2.9	
COx-EST 48599 S_{BET}=37 m^2/g, L=0.72					
ln(p/p°)	-2.1	-4.1	-6.6	-10.2	-11.5
S_i, m^2/g	8	18.8	7.6	1.8	0.8
C	5.5	38	550	$25 \cdot 10^3$	$10 \cdot 10^4$
ω	1.2	1.2	0.6	0	0
COx-EST 48601 S_{BET}=31 m^2/g, L=0.65					
Position	-2.3	-4.1	-6.5	-10.2	-11.5
S_i, m^2/g	6.6	13.2	8.7	1.7	0.7
C	7.5	38	500	$25 \cdot 10^3$	$10 \cdot 10^4$
ω	1	1.2	0.6	0	0

b – basal faces, l – lateral faces, * – bibliographic data.